


## METHODS ARTICLE

# Evaluation of ventricular–vascular coupling with critical care metrics: An in silico approach

Lawrence J. Mulligan<sup>1,2</sup>  | Justin Ungerleider<sup>2</sup> | Adam Friedman<sup>2</sup> | Benjamin Sanders<sup>2</sup> | Julian Thrash<sup>3</sup> | Daniel Ewert<sup>4</sup> | Ludmil Mitrev<sup>1,2</sup> | Jeffrey C. Hill<sup>5</sup>

<sup>1</sup>Department of Anesthesiology, Cooper University Hospital, Camden, New Jersey, USA

<sup>2</sup>Cooper Medical School of Rowan University, Camden, New Jersey, USA

<sup>3</sup>North Dakota State University, Fargo, North Dakota, USA

<sup>4</sup>University of North Dakota, Grand Forks, North Dakota, USA

<sup>5</sup>School of Medical Imaging and Therapeutics, Massachusetts College of Pharmacy and Health Sciences University, Worcester, Massachusetts, USA

## Correspondence

Lawrence J. Mulligan, Department of Anesthesiology, Cooper University Hospital, 1 Cooper Plaza, Dorrance 259, Camden 08103, NJ, USA.

Email: [mulligan-lawrence@cooperhealth.edu](mailto:mulligan-lawrence@cooperhealth.edu)

## Abstract

Mean arterial pressure and cardiac output provide insufficient guidance for the management of intraoperative hypotension (IOH). In silico models offer additional insights into acute changes in hemodynamic parameters that may be encountered during IOH. A computational model (CM) generated parameters quantifying ventricular–vascular coupling, and pressure–volume construct across levels of aortic compliance ( $C_A$ ). We studied how a loss from normal-to-stiff  $C_A$  impacts critical care metrics of hemodynamics during vascular occlusion. Pulse pressure (PP), end-systolic pressure ( $P_{es}$ ), arterial compliance (Art-ca), arterial elastance (Art-ea), and dynamic arterial elastance (Eadyn), along mechanical efficiency (ME) were measured at five levels of  $C_A$ . A loss in  $C_A$  impacted all variables. During steady-state conditions, PP,  $P_{es}$ , and stroke work increased significantly as  $C_A$  decreased. Art-ca decreased and Art-ea increased similarly; Eadyn increased and ME decreased. During a decrease in preload across all  $C_A$  levels, arterial dynamics measures remained linear. The CM demonstrated that a loss in  $C_A$  impacts measures of arterial dynamics during steady-state and transient conditions and the model demonstrates that critical care metrics are sensitive to changes in  $C_A$ . While Art-ca and Art-ea were sensitive to changes in preload, Eadyn did not change.

## KEYWORDS

aortic compliance, cardiac output, computational model, Eadyn, mechanical efficiency, pulse pressure, stroke work, ventricular–vascular coupling

## 1 | INTRODUCTION

Tools to improve intraoperative and postoperative care of patients following surgery have relied on mean arterial pressure (MAP), cardiac output (CO), systemic

vascular resistance, and pulmonary capillary wedge pressure (Awad et al., 2022; Singh & Antognini, 2011). These parameters have been shown to include an informational lag regarding the patient's hemodynamic state but remained the foundation of patient care. Recent tools have

This is an open access article under the terms of the [Creative Commons Attribution](https://creativecommons.org/licenses/by/4.0/) License, which permits use, distribution and reproduction in any medium, provided the original work is properly cited.

© 2024 The Authors. *Physiological Reports* published by Wiley Periodicals LLC on behalf of The Physiological Society and the American Physiological Society.

been developed to improve the speed and focused insight on relevant parameters. Reliance on MAP and CO to monitor intraoperative hypotension (IOH) has led to the commercial development of new parameters to provide greater insight: Baroreceptors, carotid bodies, the cardio-renal axis, and microvascular autoregulation control regulation of MAP and CO (Awad et al., 2022; Pinsky et al., 2022; Vos & Scheeren, 2019).

However, vascular aging and an accompanied loss in aortic compliance ( $C_A$ ) is not considered during management of these patients. A decrease in  $C_A$  and the resulting increase in arterial pulsatility leads to a loss of autoregulatory microvascular control, increasing the difficulty of controlling IOH (Georgianos et al., 2015; London et al., 2004; O'Rourke & Safar, 2005). Recent studies have investigated the use of Eadyn (pulse pressure [PP]/stroke volume [SV]), a dynamic version of arterial elastance ( $E_a$ ), to provide insight into IOH triage (Cecconi et al., 2015; Guarracino et al., 2013; Monge García et al., 2020).

Insight into this regulatory apparatus requires insight into how the cushion and conduit properties of the aorta impact a given patient's hemostatic level. With age, the aortic becomes less compliant, which may be coupled with a loss of the microvascular autoregulatory mechanisms and likely associated with a change in left ventricular function (Laurent et al., 2022; Laurent & Boutouyrie, 2021; Mitchell et al., 2004). The subsequent loss of cardiovascular homeostasis immediately following anesthesia induction or during the surgical case presents an additional burden to the variables listed above for the treating anesthesiologist. If the vascular tree has undergone early vascular aging (is stiffer than expected at a specific age), a loss in autoregulation will likely be more significant, and maintaining MAP within the guidelines may be more difficult.

The loss of  $C_A$  coupled with the difficulty of assessing and managing intraoperative blood pressure suggest that additional information would be helpful, and early identification and prompt management of hypotensive events can significantly impact patient outcomes (Laurent et al., 2022; Laurent & Boutouyrie, 2021). The American Society of Anesthesiologists set forth a standard rule that monitoring arterial blood pressure should not exceed an interval maximum of 5 min (Awad et al., 2022). Intraoperative blood pressure management calls for more advanced hemodynamic parameters to identify and predict patients who may experience hypotensive episodes and knowledge of  $C_A$  may improve the efficiency and use of the current monitoring paradigm.

The ventricular-vascular coupling (VVC) construct was first considered in the early work by Suga et al. (1973). The LV pressure-volume (PV) loop provided a load-independent measure of the contractile state and time-varying cardiac elastance (Kass & Kelly, 1992; Sagawa

et al., 1977). During this study, the first cardiac cycle was used to evaluate  $E_a$  ( $P_{es}/SV$ ) using the upper left-hand corner of the PV loop. Art-ea is a poor metric for evaluating VVC (Chirinos et al., 2014; Ikonomidis et al., 2019). The recently proposed parameter, dynamic arterial elastance (Eadyn), which indexes PP and SV, has been utilized in the critical care setting to predict the volume status and provide an index of compliance responsiveness of the patient (Guarracino et al., 2013; Monge García et al., 2020; Persona et al., 2022). Higher values of Eadyn ( $>1$ ) have been determined to reflect a cardiovascular system that adequately regulates blood pressure by efficiently increasing CO and arterial pressure when fluids are given (Awad et al., 2022; Guarracino et al., 2013; Monge García et al., 2020; Persona et al., 2022).

Further investigation is required to understand how Eadyn changes with manipulation of pressure and volume at different levels of  $C_A$ , simulating the “real-world” changes of loading conditions in the intensive care patient. Therefore, the aims of this study are (1) to evaluate how varying degrees of  $C_A$  impact beat-to-beat arterial compliance (Art-ca) during steady state and transient conditions, (2) to evaluate how varying degrees of  $C_A$  impact effective Art-ea, and Eadyn. To investigate these aims, a computational model (CM) previously developed was modified to include the addition of left ventricular PV with  $C_A$  values ranging from normal (baseline) to stiff (aged) and manipulation of preload via vena caval occlusions (VCOs).

## 2 | METHODS

### 2.1 | In silico computational model

A Simulink cardiopulmonary model was developed using MATLAB's MathWorks R2020b release (Natick, MA) based on previously validated work to simulate human cardiovascular experiments (Albanese et al., 2016; Cheng et al., 2016). The lumped parameter CM includes a five-compartment systemic vascular system, pulmonary circulation, mechanics, and left and right ventricles and atria. The model is hemodynamically regulated through an autonomic neurological control system and local-effect autoregulation through blood-gas concentration.

### 2.2 | Baseline model verification

The model was verified before the study by analyzing left ventricular PV loops and aortic pressures. Hemodynamic parameters of the MATLAB and Simulink model were tuned using the comparison to human physiologic cardiac PV responses seen in the work of Wiggers (Mitchell

& Wang, 2014). Under normal compliance and resistance conditions, the model generated PV waveforms with systolic, diastolic, and PP of approximately 120 mmHg, 80 mmHg, and 40 mmHg, respectively.

The model developed by Ursino et al. includes five compartments that are part of the windkessel construct but with more granularity. Instead of one lumped windkessel, Ursino's models are constructed with many distributed lumped windkessels (Albanese et al., 2016; Cheng et al., 2016). The skeletal system, brain, heart/vascular tree, splanchnic bed, extra-splanchnic, and autonomic control of blood flow to and from these compartment mimic the body's many windkessels. In the initial windkessel that Westerhof used for his first manuscript, he included a capacitor and two resistors (Westerhof et al., 1971). Today, models have a capacitor (compliance), resistance (flow resistance), and inductor (inertance).

## 2.3 | Experimental model setup

After verification, the model was adapted to fit the experimental setup and procedure of the canine experiment seen in Kelly et al. (1992). The model was modified to create the scenario used in invasive PV loop studies: right atrial pacing, autonomic nervous system (ANS) blockade, and a decrease in preload that mimics the VCO. The nominal vascular compliance and peripheral resistances were directly modified to simulate normal and stiff conditions that mimic human cardiac and arterial function and physiology (Albanese et al., 2016; Cheng et al., 2016). The model developed depicts the venous blood flow to the right atrium through the superior and inferior vena cava as the total summation of flow converging through the thoracic cavity veins. Flow convergence is modeled by

pooling the total venous blood flow from the five vascular compartments.

## 2.4 | Vena caval occlusion

Occlusion of the venous return was simulated using a time-based increase in the hemodynamic resistance of the thoracic cavity veins after allowing the system to reach a steady state 3 min before the occlusion (Figure 1). The occlusion occurred distal to the tricuspid valve and downstream of the five systemic vein sub-compartments. This in silico method is equivalent to occlusion of the vena cava via a balloon-expandable catheter delivery system that replicates a reduced venous blood flow return.

Right atrial pacing was simulated at 80 bpm across the five levels of compliance during each VCO simulation. The normal and the stiff aorta's total CA and peripheral vascular resistance ( $R_T$ ) occurred by directly modifying the cardiopulmonary model systemic arterial parameters. Due to the large variance in vascular compliance and resistance between a human arterial system and a canine subject, the original canine normal and stiff Tygon arterial parameters were modified to synchronize within the hemodynamics of the cardiopulmonary model. The Art-ca and resistances of the five compartments and aorta of the cardiopulmonary model were proportionally scaled to achieve a target equivalent compliance.

To simulate the canine arterial parameters of the Kelly et al. study in the human cardiopulmonary model, the total compliances and resistances for normal and stiff conditions were adjusted to accurately reflect physiologic human hemodynamics and were modified through proportional scaling of the arterial and aortic vascular compartments (Kelly et al., 1992). The normal canine total

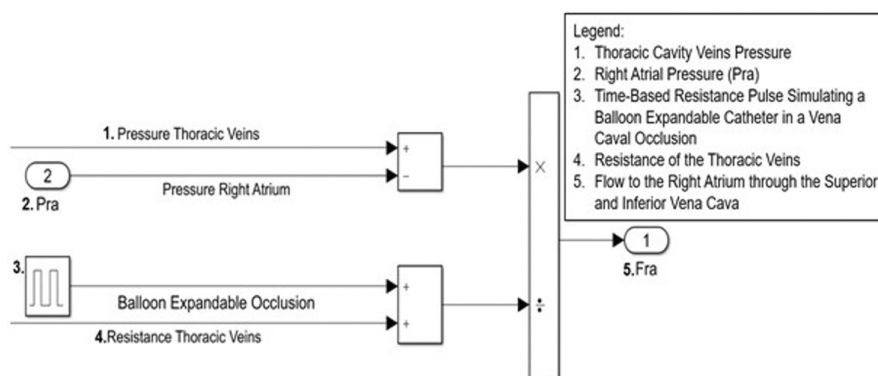


**FIGURE 1** Simulink simulated balloon expandable vena caval occlusion (VCO) method. The autonomic blockade used routinely in acute and chronic canine studies to control heart rate during 10–12 s VCO was simulated by keeping sympathetic and parasympathetic reflex signals at a constant nominal value to prevent innervation on the cardiopulmonary system during the VCO period.  $F_{ra}$ , blood flow to the right atrium;  $P_{ra}$ , pressure gradient of the thoracic veins and right atrial pressure.

compliance was directly modified from a  $C_A = 1.65 \text{ mL/mmHg}$  to  $C_A = 0.7 \text{ mL/mmHg}$  while the stiff Tygon compliance of  $C_A = 0.19 \text{ mL/mmHg}$  produced physiologically accurate hypertensive conditions within the human cardiopulmonary model. Peripheral vascular resistance was modified from the canine normal  $R_T = 3.04 \text{ mmHg.mL}^{-1}.\text{s}^{-1}$  to  $R_T = 1.28 \text{ mmHg.mL}^{-1}.\text{s}^{-1}$  while the resistance of the stiff Tygon conduit was kept at the Kelly et al. value of  $R_T = 3.66 \text{ mmHg.mL}^{-1}.\text{s}^{-1}$ .

Beat-per-beat data was collected by simulating the VCO under all levels of compliance. The results were verified through an examination of total end diastolic volume (EDV), end-systolic volume (ESV), end-systolic pressure ( $P_{es}$ ), end-diastolic pressure (EDP), PP,  $dP/dt_{\text{max}}$ , pressure-volume area (PVA), and the end-systolic pressure-volume relationship (ESPVR). Validation of the model results was conducted by comparing the hemodynamic relationships seen in previous studies (Freeman, 1990; Kelly et al., 1992; Kolh et al., 2000). Data analysis was conducted using GraphPad Prism (Boston, MA).

After calculating the normal and stiff data, the Art-ca and resistance were linearly scaled starting from the normal compliance ( $C_A = 0.7 \text{ mL/mmHg}$  and  $R_T = 1.28 \text{ mmHg.mL}^{-1}.\text{s}^{-1}$ ) and reduced to the Tygon compliance to verify the linear behavior of the cardiopulmonary model. The normal compliance  $C_A$  was decreased by 10% to  $0.63 \text{ mL/mmHg}$  and resistance of  $R_T = 1.41 \text{ mmHg.mL}^{-1}.\text{s}^{-1}$ ; then by 20% to  $C_A = 0.56 \text{ mL/mmHg}$  and  $R_T = 1.54 \text{ mmHg.mL}^{-1}.\text{s}^{-1}$ ; then by 40% to  $C_A = 0.42 \text{ mL/mmHg}$  and  $R_T = 1.805 \text{ mmHg.mL}^{-1}.\text{s}^{-1}$ ; and finally to the stiff Tygon compliance and resistance value of  $C_A = 0.19 \text{ mL/mmHg}$  and  $R_T = 3.66 \text{ mmHg.mL}^{-1}.\text{s}^{-1}$ . The model parameters and generated output are shown in Table 1.

## 2.5 | Evaluation of cardiac function

Like human and pre-clinical studies, LV volume was calculated for each beat during the simulated VCO. For the ESPVR,  $P_{es}$  and ESV were on was fit using a linear least-square algorithm to the equation:

$$P_{es} = \text{ESPVR}(E_{es} - V_o)$$

where ESPVR is the slope of the relation and  $V_o$  is its volume-axis intercept.

The PVA described by Suga et al. (1973) was calculated for each beat during the VCO. The efficiency of left ventricular energy transfer was evaluated using the method of Nozawa et al. (1988) using the equation:

$$\text{Mechanical efficiency (ME)} = (\text{SW} / \text{PVA}) \times 100$$

## 2.6 | Evaluation of arterial compliance/ elastance

The CM provided five levels of static Art-ca as described above. In addition, calculations of dynamic Art-ca ( $\text{SV}/P_{es}$ ) and Art-ea ( $P_{es}/\text{SV}$ ) were calculated. Eadyn (pulsatile “pulse pressure”/stroke volume [ $\text{PP}/\text{SV}$ ]) was also calculated. The parameters were calculated during the first beat of the VCO (steady-state) and the VCO process (transient). The CM parameters are shown in Table 1.

## 3 | RESULTS

### 3.1 | Impact of alterations in compliance on ventricular function

The changes in  $C_A$  on ventricular function variables are shown in Tables 2 and 3. The following hemodynamic changes occurred as  $C_A$  decreased from normal to stiff. The PV plane moved to the right (Figures 1 and 2), and the LV end-diastolic volumes (LVEDV) increased from 100.5 to 140.1 mL at the stiff  $C_A$ . LV end-systolic volumes (LVESV) increased from 54.1 to 87.4 during the stiff  $C_A$ , and SV increased from 46.5 to 52.7 mL (Table 2). Associated with the change in  $C_A$ , LV  $P_{es}$  increased from 81.7 mmHg at the normal setting to 133.8 mmHg during the stiff  $C_A$ . During the loss in  $C_A$ , LVEDP increased from 5.0 to 8.4 mmHg. Along with an increase in  $P_{es}$  and LVEDP, PP increased from 33.4 to 106.6 mmHg, and the changes in stroke work (SW) were also significant (3830 to 7313 mmHg mL). Measurement of left ventricular contractility with ESPVR decreased from 1.80 to 1.44 (Figure 3) during the loss in  $C_A$ . As  $C_A$  decreased, an interesting contrast occurred with the ME variable, as function of ESV. As ESV increased during the first cardiac cycle of the respective VCO, a small decrease in ME of 2% was observed. This continued to the 60%  $C_A$  setting. This was due to the increased in stroke-work, related to the increase in  $P_{es}$ . Across the five  $C_A$ 's, the change in ME during the VCO was eliminated at the Stiff setting (Table 4), beginning at 61% and ending at 60%.

### 3.2 | Impact of alterations in compliance on metrics of ventricular-vascular coupling

As expected, the loss in  $C_A$  led to similar and opposite changes in steady-state Art-ca and Art-ea (Tables 1 and 3). During the VCO maneuver, intended to mimic changes in loading condition, the change in beat-to-beat Art-ca and Art-ea was preload dependent, and the level of dependence

TABLE 1 Model parameters.

|  | Model resistance<br>( $R_T$ ) | Steady state arterial<br>compliance | Steady state arterial<br>elastance |
|--|-------------------------------|-------------------------------------|------------------------------------|
| Model compliance ( $C_A$ ) (mL/<br>mmHg) | (mmHg.mL.s <sup>-1</sup> )    | Art-ca<br>(SV/ $P_{es}$ )           | Art-ea<br>( $P_{es}$ /SV)          |
| Normal (0.7)                             | 1.28                          | 0.57                                | 1.76                               |
| 90% Normal (0.63)                        | 1.41                          | 0.50                                | 1.99                               |
| 80% Normal (0.56)                        | 1.54                          | 0.48                                | 2.08                               |
| 60% Normal (0.42)                        | 1.805                         | 0.47                                | 2.13                               |
| Stiff (0.27)                             | 3.66                          | 0.39                                | 2.54                               |

Abbreviations: Art-ca, arterial compliance; Art-ea, arterial elastance;  $C_A$ , aortic compliance;  $P_{es}$ , end-systolic pressure; SV, stroke volume.

TABLE 2 Impact of change in aortic compliance on LV function.

|                   | EDV   | ESV  | $P_{es}$ | EDP    | SW      | ESPVR     | Mech eff |
|-------------------|-------|------|----------|--------|---------|-----------|----------|
| Aortic compliance | (mL)  | (mL) | (mmHg)   | (mmHg) | mmHg.mL | (mmHg.mL) | (%)      |
| Normal            | 100.5 | 54.1 | 81.7     | 5.0    | 3830    | 1.80      | 72.2     |
| 90%               | 110.9 | 61.8 | 97.8     | 5.9    | 4802    | 1.76      | 68.6     |
| 80%               | 116.7 | 65.9 | 105.5    | 6.3    | 5359    | 1.73      | 67.4     |
| 60%               | 124.7 | 71.4 | 113.7    | 7.0    | 6150    | 1.65      | 66.4     |
| Stiff             | 140.1 | 87.4 | 133.6    | 8.4    | 7313    | 1.44      | 60.8     |

Abbreviations: EDP, end-diastolic pressure; EDV, end diastolic volume; ESPVR, end-systolic pressure–volume relationship;  $P_{es}$ , end-systolic pressure; ESV, end-systolic volume; SW, stroke work.

TABLE 3 Impact of change in aortic compliance on ventricular–vascular coupling.

| Windkessel parameters |      |       | Critical care metrics |        |       |
|-----------------------|------|-------|-----------------------|--------|-------|
| $C_A$                 | SV   | PP    | Art-ca                | Art-ea | Eadyn |
| Normal                | 46.5 | 33.4  | 0.57                  | 1.76   | 0.72  |
| 90%                   | 49.1 | 38.8  | 0.50                  | 1.99   | 0.79  |
| 80%                   | 50.8 | 44.0  | 0.48                  | 2.08   | 0.87  |
| 60%                   | 53.3 | 56.0  | 0.47                  | 2.13   | 1.05  |
| Stiff                 | 52.7 | 106.6 | 0.39                  | 2.53   | 2.02  |

Abbreviations: Art-ca, arterial compliance; Art-ea, arterial elastance;  $C_A$ , aortic compliance; Eadyn, dynamic arterial elastance; PP, pulse pressure; SV, stroke volume.

decreased as  $C_A$  decreased (Figures 4 and 5). However, the impact of the preload maneuver did not have the same effects on Eadyn (Figure 6). Eadyn uses PP, and Art-ca and Art-ea use  $P_{es}$ . We evaluated the relationship between stroke volume and the two pressures at each  $C_A$  during the VCO (Figures 7 and 8). Eadyn remained linear but was not preload-dependent. The relationship between PP and  $P_{es}$  was not linear (Figure 9) at any level  $C_A$ . The impact of a loss in  $C_A$  on ME provided new observations. From the

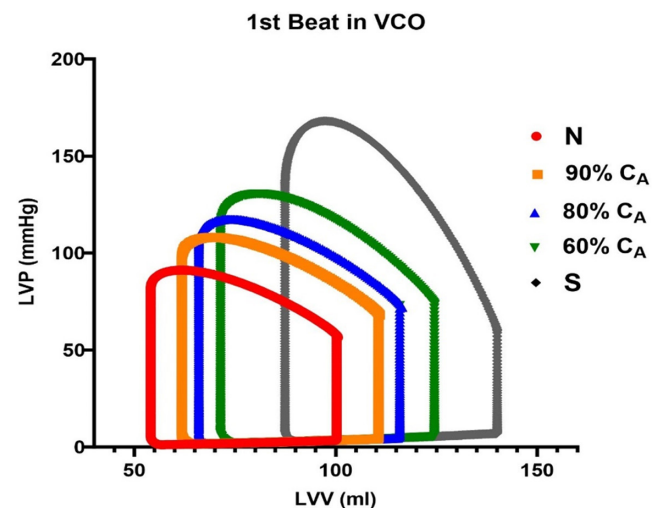
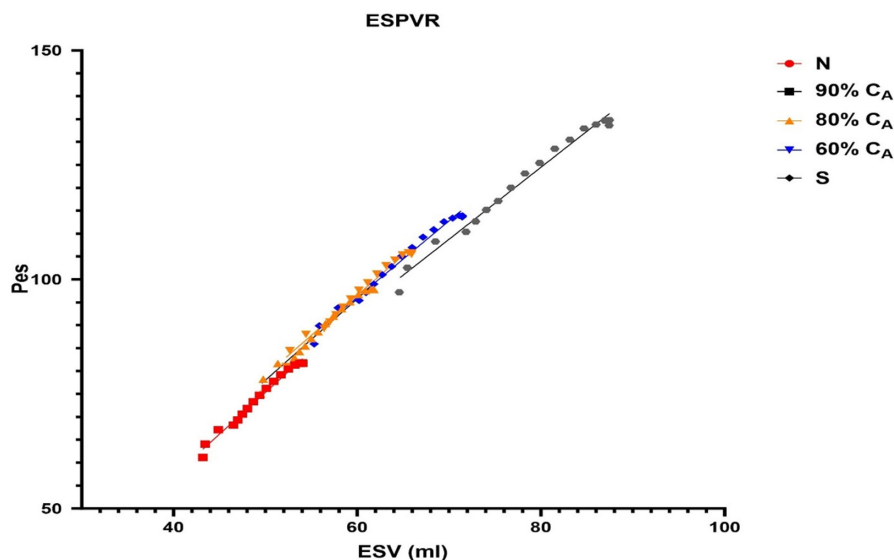


FIGURE 2 The impact of a loss in aortic compliance on steady state cardiac function. The first cardiac cycle from the vena caval occlusion (VCO) maneuver for each compliance is shown with each loop moving to the right. LVP, left ventricular pressure; LVV, left ventricular volume.

normal setting of  $C_A$  to the stiff setting, a loss in ME of 20% was observed (72%–61%) at steady state. During the VCO, the impact of a loss in  $C_A$  on ME increased. By the stiff



**FIGURE 3** The impact of a loss in aortic compliance on end-systolic pressure–volume relationship (ESPVR). The data were collected during a vena caval occlusion (VCO) maneuver for each compliance. The slopes are similar but there was a small reduction in ESPVR at the stiff aortic compliance ( $C_A$ ) (see Section 4).

|                        | Normal | 90% | 80% | 60% | Stiff |
|------------------------|--------|-----|-----|-----|-------|
| First cardiac cycle-ME | 72%    | 69% | 67% | 67% | 61%   |
| Last cardiac cycle-ME  | 61%    | 59% | 59% | 59% | 60%   |

**TABLE 4** Impact of change in aortic compliance on mechanical efficiency during a vena caval occlusion.

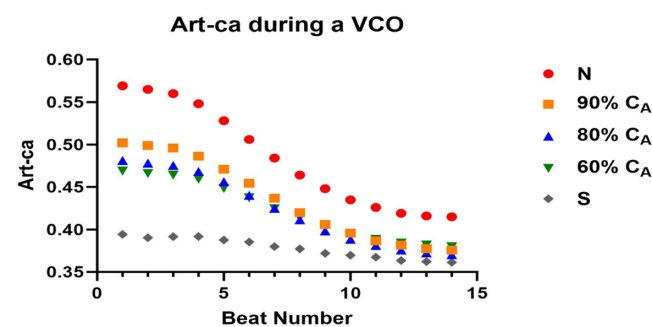


**FIGURE 4** The impact of a loss in aortic compliance ( $C_A$ ) on the transient arterial compliance (Art-ca) during a vena caval occlusion (VCO).

setting, there was no change in ME, which was in contrast to the other settings (Table 4).

## 4 | DISCUSSION

The in silico CM was modified to evaluate four questions: (1) Does a loss in  $C_A$  impact the left ventricular PV-derived variables? (2) Does a loss in  $C_A$  impact variables representing VVC? (3) Does the loss in ( $C_A$ ) impact the clinically focused critical care metric, Eadyn along with Art-ca? And is (4) Eadyn responsive to changes in preload? To accomplish this, we used a lumped parameter approach. The model was modified to provide insights from the left ventricular PV plane during alterations in

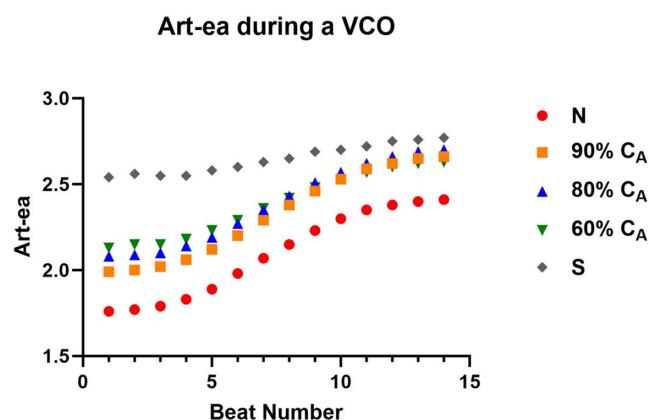


**FIGURE 5** The impact of a loss in aortic compliance ( $C_A$ ) on transient effective arterial elastance (Art-ea) during a vena caval occlusion (VCO).

preload and afterload. The four objectives were achieved, and the PV loop data generated by the model are in agreement with previous in vivo studies. These findings provide a critical appraisal of tools used in the critical care setting.

The model developed by Ursino et al. includes five compartments that are part of the windkessel construct but with more granularity. Instead of one lumped windkessel, Ursino's models are constructed with a distributed lumped windkessel approach (Albanese et al., 2016; Cheng et al., 2016; Little et al., 1989). The skeletal system, brain, heart/vascular tree, splanchnic bed, extra-splanchnic and autonomic control of blood flow to and from these

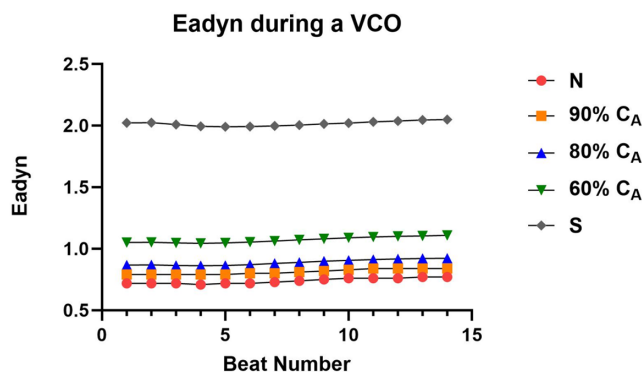


**FIGURE 6** The impact of a loss in aortic compliance ( $C_A$ ) on the transient dynamic arterial elastance (Eadyn) during a vena caval occlusion (VCO).

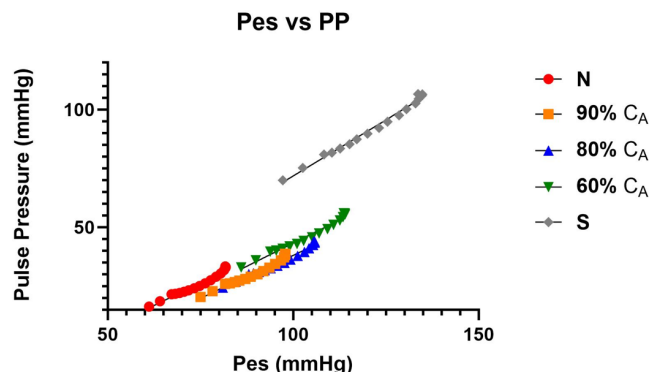


**FIGURE 9** Relationship between end-systolic pressure (ESP) and pulse pressure (PP) during vena caval occlusions (VCOs) at the five levels of aortic compliance ( $C_A$ ).

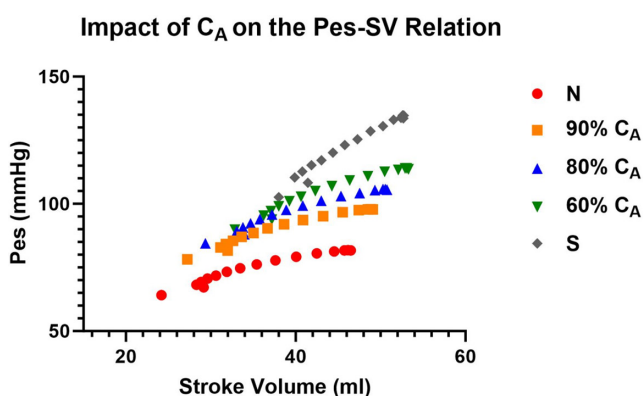


**FIGURE 7** The impact of a loss in aortic compliance ( $C_A$ ) on the end-systolic pressure ( $P_{es}$ )–stroke volume relation during a vena caval occlusion (VCO).

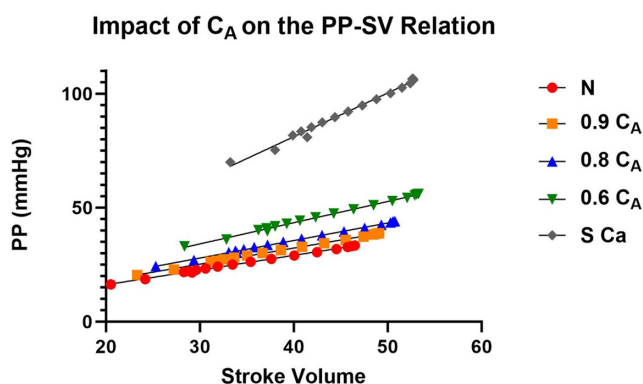


**FIGURE 8** The impact of a loss in aortic compliance ( $C_A$ ) on the pulse pressure (PP)–stroke volume (SV) relation during a vena caval occlusion (VCO).

compartments mimic the circulation's windkessels. In the initial windkessel work by Westerhof, the model included a capacitor and two resistors. Today, models have

a capacitor (compliance), resistance (flow resistance) and inductor (inertance).

#### 4.1 | Impact of vascular aging on cardiac function

The CM produced data that suggest the following: first the model produced PV loops measured during the first beat in a VCO that displayed the expected rightward shift along the left ventricular volume axis as  $C_A$  decreased, second, the loss in  $C_A$  resulted in a graded response, providing insight into how the loss of  $C_A$  may impact cardiac function and finally, the existing metrics to evaluate response to preload maneuvers and subsequent changes in PP responded to changes in preload while Eadyn did not. The steady-state loss in  $C_A$  also led to increases in LVESV, LVEDP, PP, SV, and SW. Along with the changes in volumes and left ventricular pressures during the loss in  $C_A$ , ESPVR decreased slightly from 1.80 to 1.44, along with a steady loss in ME.

#### 4.2 | Impact of vascular on VVC

The CM allowed for an investigation of VVC across a wide range of vascular compliances. As Eadyn has been linked to changes in arterial stiffness or compliance, we investigated the impact of simulated vascular aging on cardiac and vascular function. From the PV construct, we determined that the CM behaved in a manner similar to pre-clinical and clinical studies regarding cardiac function, preload, ME and contractility (Chen et al., 1998; Freeman, 1990; Kolh et al., 2000). Using the CM, we evaluated how Art-Ca, Art-ea and Eadyn responded at five levels of  $C_A$ . The steady-state data suggest that Art-ca and Art-ea parameters behave as expected as  $C_A$  decreases

in vascular aging (Table 3). Eadyn also changes during steady-state conditions, as  $C_A$  decreased Eadyn increased from 0.72 to 2.02.

During the VCO, Art-ca and Art-ea behaved in an inverse manner (Figures 4 and 5). The Eadyn construct suggests that VVC is good or optimal above a value of 1.0. The CM showed that a normal  $C_A$  was associated with a value of 0.72 and only when the CM simulated a stiff vascular bed, did Eadyn rise above 1.0. The normal  $C_A$  for ESPVR and ME are aligned with human values, while the Eadyn value of 0.72 is 50% of that measured in patients with an average ejection fraction of 54% (Kameyama et al., 1992).

Our observation regarding Eadyn may be a function of the model. The other parameters from the PV construct are aligned with previous studies and the behavior of Art-ea is also aligned. During the VCO, new observations include a dynamic response of Art-ca and Art-ea (Figures 4 and 5) that mirror each other and a lack of a response in Eadyn (Figure 6). The cause of this difference is likely the use of PP in the Eadyn tool versus  $P_{es}$  (Figures 7 and 8) where stroke volume on the x-axis is the common element. The slopes and intercepts appear to be quite different between PP and  $P_{es}$ . In the Monge-Garcia dataset, Art-ea is 1.29 at baseline and 0.80 following phenylephrine with a reverse during sodium nitroprusside (1.13–2.0). These data are from animal models, while the CM mimics human data, but the Eadyn findings during the phenylephrine and sodium nitroprusside decreased from 1.51 to 0.98 and increased from 1.36 to 1.79. This suggests that during phenylephrine, PP decreased more than SV while during nitroprusside SV increased more than PP.

The Eadyn parameter was intended to provide insight using critical care parameters to guide decision-making in patients who may require volume. As  $C_A$  decreases with age, the PP increases, and the long-term increase in afterload leads to a loss in SV. In the CM, left ventricular function remains normal, enabling the study to address vascular aging only. This resulted in a significant increase in PP and a larger Eadyn than would be seen in a critical care patient. By modifying the model proposed by Albanese et al. (2016), we were able to investigate how the loss in  $C_A$  impacted Eadyn. The Eadyn variable was based on the effective arterial elastance ( $E_a$  or Art-ea) construct. In the PV construct,  $E_a$  is only considered for the first cardiac cycle of the PV loop data, and this is due to  $E_a$  changing during the VCO and, therefore, cannot represent the Art-ea similar to ventricular elastance. However, Eadyn was intended to evaluate pulsatile changes in SV and PP.

The premise of Eadyn was to determine if a patient would be responsive to fluids. The addition of fluids would

be expected to change preload, MAP, and stroke volume in a homeostatic circulation. The VCO maneuver has been shown to drop preload and afterload without changing sympathetic control of the circulation. The CM VCO provided a close similarity to this technique.

In contrast to the relationship between Eadyn and Art-ca, we investigated how the loss of  $C_A$  impacted the beat-to-beat change in both Art-ea and Eadyn during the VCO, respectively (Figures 5 and 6). During a VCO, the characterization ESPVR is linear, providing the load-independent measure of contractile function. However, the changes in the vascular side ( $E_a$ ) are not linear. In Figures 4 and 5, the impact of a loss in  $C_A$  is clear, and the impact of the loss on Art-ca and Art-es during the VCO, as the vascular tree stiffens, is clear. The consequences of this behavior are two-fold. First, the need to move away from effective arterial elastance ( $E_a$ , Art-ea) as part of the VVC paradigm is clear and recent work provides the basis for this (Chirinos et al., 2014).  $E_a$  is used only during steady state conditions and depends on heart rate and peripheral resistance as is  $C_A$ . Second, the change in beat-to-beat Art-ca during a VCO is evident at the five levels of  $C_A$ . This evidence supports the load dependence of assessing VVC across the spectrum of vascular aging.

### 4.3 | Comparison of arterial elastance/compliance with Eadyn

The transition of the use of  $E_a$  to Eadyn includes the use of PP compared with  $P_{es}$ . Physiologically, the use of PP adds to the complexity as PP is known to increase with vascular aging (Chen et al., 1998; Chirinos, 2022; Climie et al., 2023; London et al., 2004). In addition, the relationship between change in PP and stroke volume during the process of vascular aging is complicated. As the Eadyn metric calculates stroke volume from the radial arterial pressure line, it is reasonable to conclude that in the patient population over 50 years, which was simulated to a degree at the 60% and stiff settings, an error may develop in the metric.

We were interested in how the change in  $C_A$  impacted Art-ca. In Figure 4, a loss in  $C_A$  from normal to stiff led to a lower value and the contrast of the beat-to-beat decline demonstrates the load dependence of the variable. Evaluation of Eadyn showed a lack of change as  $C_A$  decreased, suggesting the lack of sensitivity of parameter. The relationship between  $P_{es}$  and stroke volume was curvilinear remained linear (Figure 7) but the relationship between PP and stroke volume was linear. Also, the impact of a loss in  $C_A$  led to gradual separation in the relationship while the loss in  $C_A$  created similar slopes but greater separation with PP (Figure 8).

#### 4.4 | Model limitations

The major limitation of the study is the use of a CM to stimulate the human cardiovascular system compared to the use of human subjects. Due to the invasive and specific nature of the parameters being measured (Art-ca, ESPVR, SV, and ME) and the use of a change in loading conditions across degrees of vascular aging, utilizing human subjects is not possible. The initial focus of the model was to simulate vascular aging with a normal heart. The next step could focus on changing the function of the heart in a similar manner both with and without disease. Invasive studies in a large sample of patients aged 25–75 years to generate the VVC and Art-ca data who are undergoing cardiac catheterization or cardiac surgery is not realistic. Other have used in vivo and in silico methods to evaluate similar questions (Moulton & Secomb, 2023; Pagoulatou et al., 2021; Pagoulatou & Stergiopoulos, 2017). Modeling these hemodynamic situations at varying  $C_A$ s and preloads served as a reasonable and effective way to assess Eadyn. Extrapolating these data and the associated relationship in human subjects is an opportunity to improve the validity and better understand the potential clinical utility. A possible next step would be to use human models with varying degrees of aortic stiffness and volume status to assess Eadyn, and ultimately the relationship to predicting fluid responsiveness. As Eadyn continues to become more accessible, less invasive and a standard part of anesthesia practice, future studies can involve human subjects to better relate this information to the human cardiovascular system as opposed to simulation via CMs.

## 5 | CONCLUSION

The development of noninvasive or minimally invasive tools for assessing fluid responsiveness in surgical patients continues to build on fundamental hemodynamics. The creation of Eadyn as tool to assist with this goal appears to provide important guidance regarding patient volume status. However, the degree of vascular aging, minimal to severe, that may have developed in the patient, can impact the responsiveness of this variable, as the computational model has demonstrated.

#### FUNDING INFORMATION

The authors declare that this report did not receive any specific grant from public, commercial, or not-for-profit funding agencies.

#### DATA AVAILABILITY STATEMENT


Julian Thrash can be reached out at [julian.thrash@ndsu.edu](mailto:julian.thrash@ndsu.edu) for further information on the CM model and code

used to modify the CM. Questions regarding the datasets can be directed to Larry Mulligan at [mulligan-lawrence@cooperhealth.edu](mailto:mulligan-lawrence@cooperhealth.edu).

#### ETHICAL APPROVAL

The authors declare that the work described has been carried out in accordance with The Code of Ethics of the World Medical Association (Declaration of Helsinki) for experiments involving humans. There were no human subjects included in this study.

#### ORCID

Lawrence J. Mulligan  <https://orcid.org/0000-0002-1868-0150>

#### REFERENCES

- Albanese, A., Cheng, L., Ursino, M., & Chbat, N. W. (2016). An integrated mathematical model of the human cardiopulmonary system: Model development. *American Journal of Physiology. Heart and Circulatory Physiology*, 310(7), H899–H921.
- Awad, H., Alcodray, G., Raza, A., Boulos, R., Essandoh, M., Bhandary, S., & Dalton, R. (2022). Intraoperative hypotension-physiologic basis and future directions. *Journal of Cardiothoracic and Vascular Anesthesia*, 36(7), 2154–2163.
- Cecconi, M., Monge García, M. I., Gracia Romero, M., Mellinshoff, J., Caliendo, F., Grounds, R. M., & Rhodes, A. (2015). The use of pulse pressure variation and stroke volume variation in spontaneously breathing patients to assess dynamic arterial elastance and to predict arterial pressure response to fluid administration. *Anesthesia and Analgesia*, 120(1), 76–84.
- Chen, C. H., Nakayama, M., Nevo, E., Fetis, B. J., Maughan, W. L., & Kass, D. A. (1998). Coupled systolic-ventricular and vascular stiffening with age: Implications for pressure regulation and cardiac reserve in the elderly. *Journal of the American College of Cardiology*, 32(5), 1221–1227.
- Cheng, L., Albanese, A., Ursino, M., & Chbat, N. W. (2016). An integrated mathematical model of the human cardiopulmonary system: Model validation under hypercapnia and hypoxia. *American Journal of Physiology. Heart and Circulatory Physiology*, 310(7), H922–H937.
- Chirinos, J. A. (2022). Ventricular-arterial coupling in heart failure: Time to close the loop and catch the wave? *JACC: Cardiovascular Imaging*, 15(9), 1560–1562.
- Chirinos, J. A., Rietzschel, E. R., Shiva-Kumar, P., De Buyzere, M. L., Zamani, P., Claessens, T., Geraci, S., Konda, P., De Bacquer, D., Akers, S. R., Gillebert, T. C., & Segers, P. (2014). Effective arterial elastance is insensitive to pulsatile arterial load. *Hypertension*, 64(5), 1022–1031.
- Climie, R. E., Alastruey, J., Mayer, C. C., Schwarz, A., Laucyte-Cibulskiene, A., Voicehovska, J., Bianchini, E., Bruno, R. M., Charlton, P. H., Grillo, A., Guala, A., Hallab, M., Hametner, B., Jankowski, P., Königstein, K., Lebedeva, A., Mozos, I., Pucci, G., Puzantian, H., ... Weber, T. (2023). Vascular ageing—moving from bench towards bedside. *European Journal of Preventive Cardiology*, 30, 1101–1117.
- Freeman, G. L. (1990). Effects of increased afterload on left ventricular function in closed-chest dogs. *The American Journal of Physiology*, 259(2 Pt 2), H619–H625.

- Georgianos, P. I., Sarafidis, P. A., & Liakopoulos, V. (2015). Arterial stiffness: A novel risk factor for kidney injury progression? *American Journal of Hypertension*, 28(8), 958–965.
- Guarracino, F., Baldassarri, R., & Pinsky, M. R. (2013). Ventriculo-arterial decoupling in acutely altered hemodynamic states. *Critical Care*, 17(2), 213.
- Ikonomidis, I., Aboyans, V., Blacher, J., Brodmann, M., Brutsaert, D. L., Chirinos, J. A., De Carlo, M., Delgado, V., Lancellotti, P., Lekakis, J., Mohty, D., Nihoyannopoulos, P., Parissis, J., Rizzoni, D., Ruschitzka, F., Seferovic, P., Stabile, E., Tousoulis, D., Vinereanu, D., ... Metra, M. (2019). The role of ventricular-arterial coupling in cardiac disease and heart failure: Assessment, clinical implications and therapeutic interventions. A consensus document of the European Society of Cardiology Working Group on Aorta & Peripheral Vascular Diseases, European Association of Cardiovascular Imaging, and heart failure association. *European Journal of Heart Failure*, 21(4), 402–424.
- Kameyama, T., Asanoi, H., Ishizaka, S., Yamanishi, K., Fujita, M., & Sasayama, S. (1992). Energy conversion efficiency in human left ventricle. *Circulation*, 85(3), 988–996.
- Kass, D. A., & Kelly, R. P. (1992). Ventriculo-arterial coupling: Concepts, assumptions, and applications. *Annals of Biomedical Engineering*, 20(1), 41–62.
- Kelly, R. P., Tunin, R., & Kass, D. A. (1992). Effect of reduced aortic compliance on cardiac efficiency and contractile function of in situ canine left ventricle. *Circulation Research*, 71(3), 490–502.
- Kolh, P., D'Orio, V., Lambermont, B., Gerard, P., Gommès, C., & Limet, R. (2000). Increased aortic compliance maintains left ventricular performance at lower energetic cost. *European Journal of Cardio-Thoracic Surgery*, 17(3), 272–278.
- Laurent, S., Agabiti-Rosei, C., Bruno, R. M., & Rizzoni, D. (2022). Microcirculation and macrocirculation in hypertension: A dangerous cross-link? *Hypertension*, 79(3), 479–490.
- Laurent, S., & Boutouyrie, P. (2021). Vascular ageing—state of play, gaps and key issues. *Heart, Lung & Circulation*, 30(11), 1591–1594.
- Little, W. C., Cheng, C. P., Mumma, M., Igarashi, Y., Vinten-Johansen, J., & Johnston, W. E. (1989). Comparison of measures of left ventricular contractile performance derived from pressure-volume loops in conscious dogs. *Circulation*, 80(5), 1378–1387.
- London, G. M., Marchais, S. J., Guerin, A. P., & Pannier, B. (2004). Arterial stiffness: Pathophysiology and clinical impact. *Clinical and Experimental Hypertension*, 26(7–8), 689–699.
- Mitchell, G. F., Parise, H., Benjamin, E. J., Larson, M. G., Keyes, M. J., Vita, J. A., Vasan, R. S., & Levy, D. (2004). Changes in arterial stiffness and wave reflection with advancing age in healthy men and women: The Framingham Heart study. *Hypertension*, 43(6), 1239–1245.
- Mitchell, J. R., & Wang, J. J. (2014). Expanding application of the Wiggers diagram to teach cardiovascular physiology. *Advances in Physiology Education*, 38(2), 170–175.
- Monge García, M. I., Jian, Z., Hatib, F., Settels, J. J., Cecconi, M., & Pinsky, M. R. (2020). Dynamic arterial elastance as a ventriculo-arterial coupling index: An experimental animal study. *Frontiers in Physiology*, 11, 284.
- Moulton, M. J., & Secomb, T. W. (2023). A fast computational model for circulatory dynamics: Effects of left ventricle-aorta coupling. *Biomechanics and Modeling in Mechanobiology*, 22(3), 947–959.
- Nozawa, T., Yasumura, Y., Futaki, S., Tanaka, N., Uenishi, M., & Suga, H. (1988). Efficiencies from consumed O<sub>2</sub> and pressure-volume area to work of in situ dog heart. *The Japanese journal of physiology*, 38(5), 713–728.
- O'Rourke, M. F., & Safar, M. E. (2005). Relationship between aortic stiffening and microvascular disease in brain and kidney: Cause and logic of therapy. *Hypertension*, 46(1), 200–204.
- Pagoulatou, S., Adamopoulos, D., Rovas, G., Bikia, V., & Stergiopoulos, N. (2021). The effect of left ventricular contractility on arterial hemodynamics: A model-based investigation. *PLoS One*, 16(8), e0255561.
- Pagoulatou, S., & Stergiopoulos, N. (2017). Evolution of aortic pressure during normal ageing: A model-based study. *PLoS One*, 12(7), e0182173.
- Persona, P., Tonetti, T., Valeri, I., Pivetta, E., Zarantonello, F., Pettenuzzo, T., De Cassai, A., & Navalesi, P. (2022). Dynamic arterial elastance to predict mean arterial pressure decrease after reduction of vasopressor in septic shock patients. *Life (Basel)*, 13(1), 28.
- Pinsky, M. R., Cecconi, M., Chew, M. S., De Backer, D., Douglas, I., Edwards, M., Hamzaoui, O., Hernandez, G., Martin, G., Monnet, X., Saugel, B., Scheeren, T. W. L., Teboul, J. L., & Vincent, J. L. (2022). Effective hemodynamic monitoring. *Critical Care*, 26(1), 294.
- Sagawa, K., Suga, H., Shoukas, A. A., & Bakalar, K. M. (1977). End-systolic pressure/volume ratio: A new index of ventricular contractility. *The American Journal of Cardiology*, 40(5), 748–753.
- Singh, A., & Antognini, J. F. (2011). Perioperative hypotension and myocardial ischemia: Diagnostic and therapeutic approaches. *Annals of Cardiac Anaesthesia*, 14(2), 127–132.
- Suga, H., Sagawa, K., & Shoukas, A. A. (1973). Load independence of the instantaneous pressure-volume ratio of the canine left ventricle and effects of epinephrine and heart rate on the ratio. *Circulation Research*, 32(3), 314–322.
- Vos, J. J., & Scheeren, T. W. L. (2019). Intraoperative hypotension and its prediction. *Indian Journal of Anaesthesia*, 63(11), 877–885.
- Westerhof, N., Elzinga, G., & Sipkema, P. (1971). An artificial arterial system for pumping hearts. *Journal of Applied Physiology*, 31(5), 776–781.

**How to cite this article:** Mulligan, L. J., Ungerleider, J., Friedman, A., Sanders, B., Thrash, J., Ewert, D., Mitrev, L., & Hill, J. C. (2024). Evaluation of ventricular-vascular coupling with critical care metrics: An in silico approach. *Physiological Reports*, 12, e15920. <https://doi.org/10.14814/phy2.15920>